

International Conference on Space Optics—ICSO 2022

Dubrovnik, Croatia

3–7 October 2022

Edited by Kyriaki Minoglou, Nikos Karafolas, and Bruno Cugny,



Remanence characterization of NGP detector in SWIR bands



Remanence characterization of NGP detector in SWIR bands

J-M. Gaucel*^a, A. Lefebure ^a, A. Gaucher^b, G. Bouchage^b, E. Sanson^b

^aThales Alenia Space, 5 All. des Gabians, Cannes la Bocca, FRANCE; ^bLynred 364 Avenue de Valence, Actipole CS 10021, 38113 Veurey-Voroize, France

ABSTRACT

Within the framework of the ESA Copernicus Carbon Dioxide Monitoring (CO2M) mission, the Short-wave infrared (SWIR) Next-Generation Panchromatic (NGP) detector, designed and manufactured by Lynred, has been extensively characterized to assess its suitability for the mission. We present here the results of the remanence measurement tests, as well as the exploitation of the data, carried out on the detector, using a bench dedicated to the measurement of remanence.

This characterization made it possible to identify three remanence effects, two are linked to the ROIC and one linked to the sensitive layer effect. We demonstrated that the ROIC effects, are, respectively, removed, by the use of a non-destructive reading for the first, and by a slight increase of the reset time for the second.

The third effect, the LAG, has been characterized with a very high accuracy (better than two electrons). This characterization shows that the LAG is fully linear with the illumination magnitude. This allowed us to build a numerical correction model that has been tested on real data. Using real measurement data, the residuals after correction are assessed lower than 10 electrons.

The purpose of this test campaign, and among others the results presented here, made it possible to demonstrate the feasibility of the CO2M mission using the NGP detector. This feasibility was difficult to obtain because the main instrument of the CO2M satellite, named CO2I, is very sensitive to remanence, especially when it is nonlinear with illumination magnitude.

If the measurements and the design of the test bench were made by Thales Alenia Space, this work is part of a collaborative technical work between Thales Alenia Space, Lynred, and the European Space Agency.

Keywords: detector, SWIR, NGP, LAG, remanence, numerical correction, ground characterization, CO2M.

1. INTRODUCTION

Within the framework of the ESA Copernicus Carbon Dioxide Monitoring (CO2M) mission [1], the Short-wave infrared (SWIR) Next-Generation Panchromatic (NGP) detector has been identified as a good choice for the main instrument CO2I.

NGP is the first large format SWIR flight model in a class higher than 1k² developed by a European firm, lynred [2]:

- It covers wavelengths of interest in the SWIR region, corresponding to the absorption of different elements present in the atmosphere (e.g. CO₂, NO_x, CH₄, etc.)
- The format is well suited to meet the current requirements of spectro-imager instruments, notably the swath cover (the area imaged on the Earth's surface) as well as the spectral resolution
- Radiometric performances are also well adapted to meet the signal-to-noise ratio parameters of the atmosphere chemistry applications required, such as in the CO2M mission

Flight models of NGP are currently deployed in instruments onboard other environmental space observation missions, showing the remarkable performance and reliability of this high-end large format SWIR detector. These missions include the Sentinel 5 ESA instrument onboard the METOP-SG platform and the French space agency CNES' Microcarb.

Beyond the classic constraints relating to the choice of the detector, for the CO2I instrument, a major constraint concerns the remanence. This constraint is expressed along two axes, a first axis concerns the amplitude of this one, and the second axis concerns the linearity of the phenomenon as a function of the illumination flux. The concern about

remanence is linked to a trapping-detrapping phenomenon that has been observed and characterized on other detectors [3].

2. REMANENCE CHARACTERIZATION MAIN CHARACTERISTICS

The test bench uses a total illumination of the detector with a partial homogeneity. On the light path is inserted a shutter that allows to quickly switch from a lighted scene to a dark scene.

The remanence is characterized on the samples after the transitions (either the rising edge or the falling edge).

The scenario number 23 has been used for the characterizations. The chronogram of this scenario is presented on the Figure 1 where the main parameters are:

- The number of readings with the shutter open: $N = 9$
- The number of readings with the shutter close: $M = 11$
- The number of cycles: $P = 56$

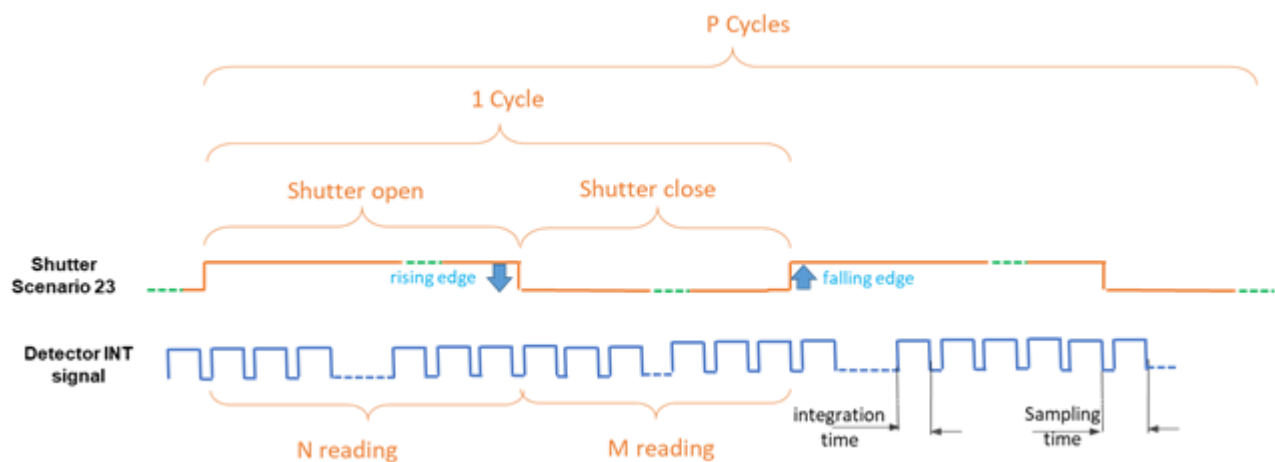


Figure 1. Remanence characterization scenario 23

The test bench main characteristics are:

- Conversion factor : 1 lsb ~ 10 electrons
- Chain Offset + background = 1400lsb
- Dark current @ 150K : ~ 2000e- /Tsamp (~1/3s)
- Total offset ~ 1600lsb
- ANC 16 bits -> High Mesurable integrated flux : 650 ke- ($2^{16} * 10 e^-$)
- 650ke- is the approximate saturation

Detector test configuration:

- Reading mode : ITR
- 7.352 MHz
- Sampling time = 308ms
- Reset time = 37.2 ms

3. OBSERVED INTER-FRAME REMANENCE

There are three inter-frame effects identified, and named the LAG, the Reset memory offset and the Negative offset.

The 3 effects are pixel-to-pixel effects. There is no spatial impact.

The Reset memory offset and the Negative offset have an impact from the previous frame on the current. These two effects are due to parasite capacity in the ReadOut Integrated Circuit (ROIC).

The third effect, the LAG have a stabilization period longer than three frames. It is a sensitive layer effect.

The Figure 2 give an illustration of these effect.

The purpose of these tests is to detect phenomena and isolate them in order to characterize them precisely.

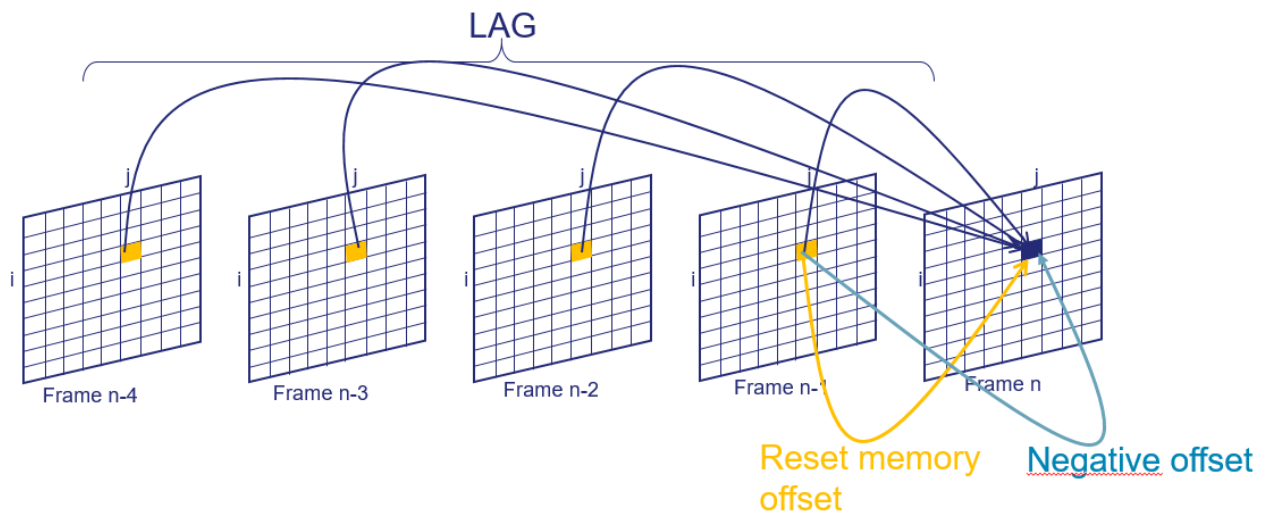


Figure 2: Illustration of the impact of the three Inter frame effects.

4. INTER FRAME EFFECT - NEGATIVE OFFSET

The characterization method used to characterize the negative offset is specific to it, and use a 4-reading mode (it means 4 reading during the sampling time).

Two illustrations of the measurement of this effect are given in the Figure 3 and the Figure 4. This measurement have been done for various magnitude of the Light to Dark transition, allowing to modeling the magnitude of the effect:

$$\text{NegativeOffset} = -2.5e-3 * \text{LDmagnitude} - 80 \text{ [electron]}$$

Where LDmagnitude is the magnitude in electron of the Light to Dark transition.

Starting from the second, the reading is offset free of this effect. This effect is not present after a dark to light transition.

For all the following measurements, we will acquire in double reading, and will use only the second reading in order to be free of the negative offset.

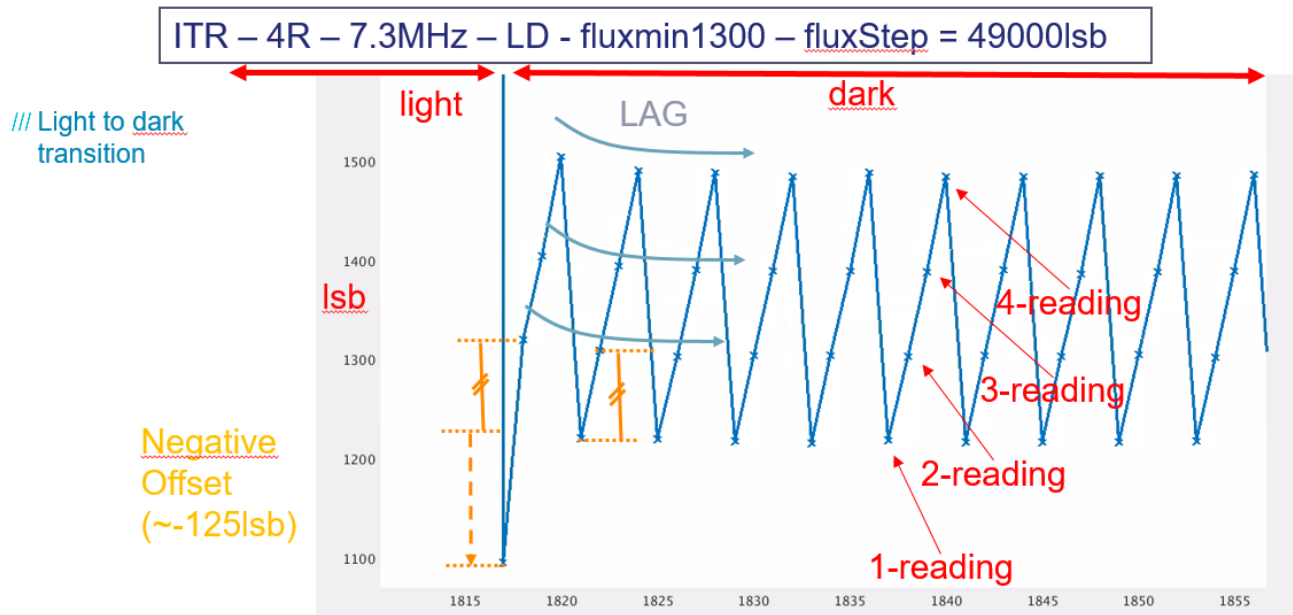


Figure 3. measurement in 4 reading mode in order to assess the negative offset with a high flux step

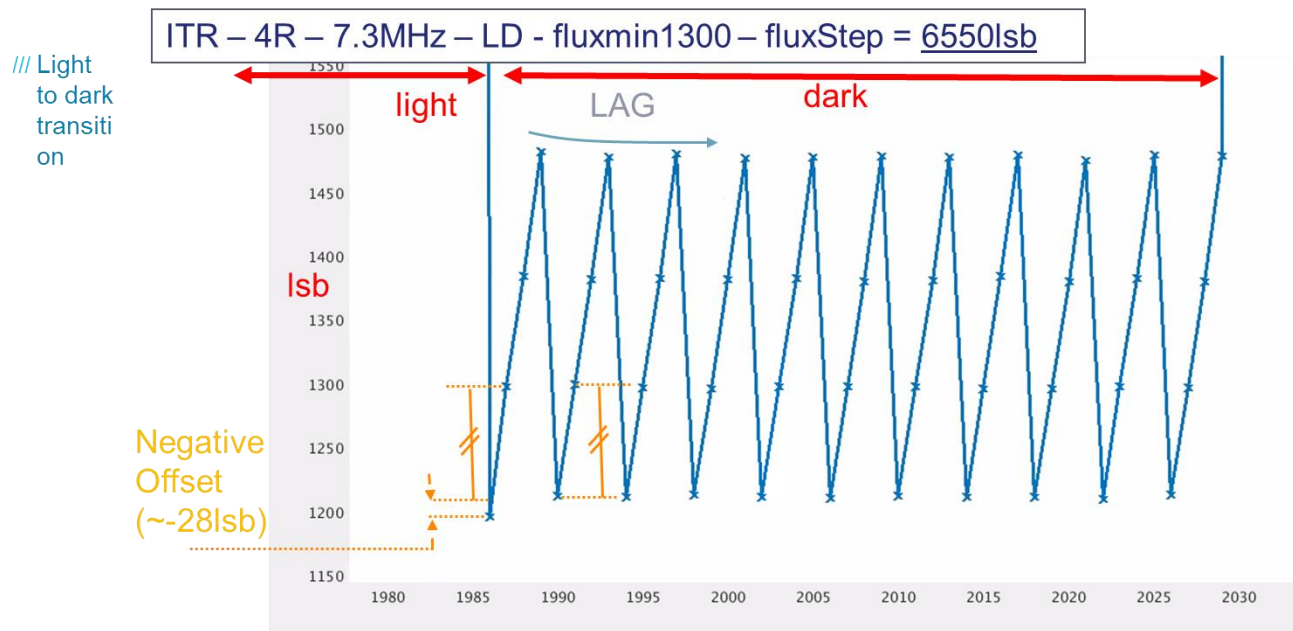


Figure 4. measurement in 4 reading mode in order to assess the negative offset with a low flux step

5. INTER FRAME EFFECT - RESET MEMORY OFFSET

This is an effect from the frame n-1 to the frame n.

The magnitude of the effect depends on:

- the reset time
- the magnitude of the transition.

The following Figure 5 gives synthetic representation of the results. The two main conclusions are :

- This effect is nonlinear with transition magnitude.
- This effect can be avoid using a sufficient reset time.

In our configuration the chosen reset time is 37.2ms and used for the following measurement. Note that the remanence effect from the frame n-1 to the frame n, showed in the Figure 5, is not reduce to zero, and is going to be study in the last part of this article.

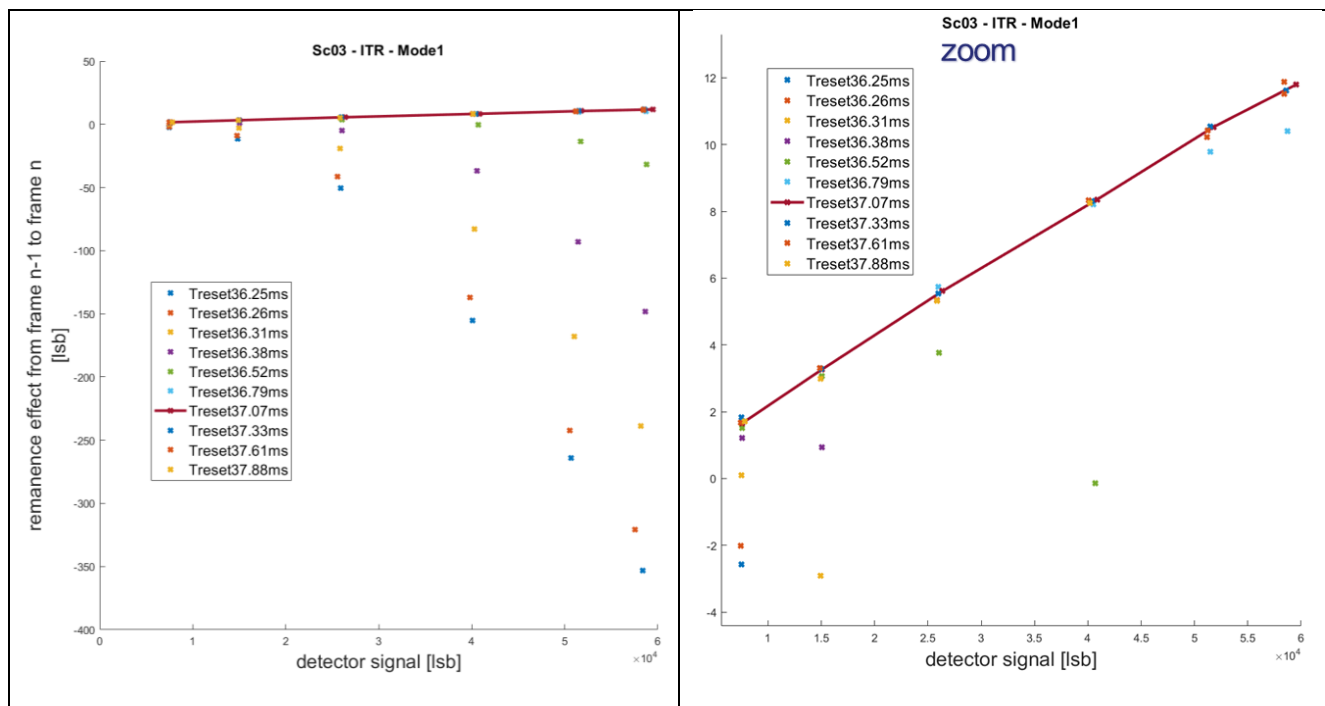


Figure 5. (The showed time reset include reading time equals to 36.21ms in our configuration).

6. INTER FRAME EFFECT – LAG

The LAG is a sensitive layer effect. It have a impact from the frame n-1 to frame n/n+1/n+2 ...

6.1 Raw Measurements

The following Figure 6 shows the raw LAG measurements after a light to dark transition (top) and after a dark to light transition (bottom), for various magnitude of the transition.

After typically 7 Sampling time, the LAG is totally removed.

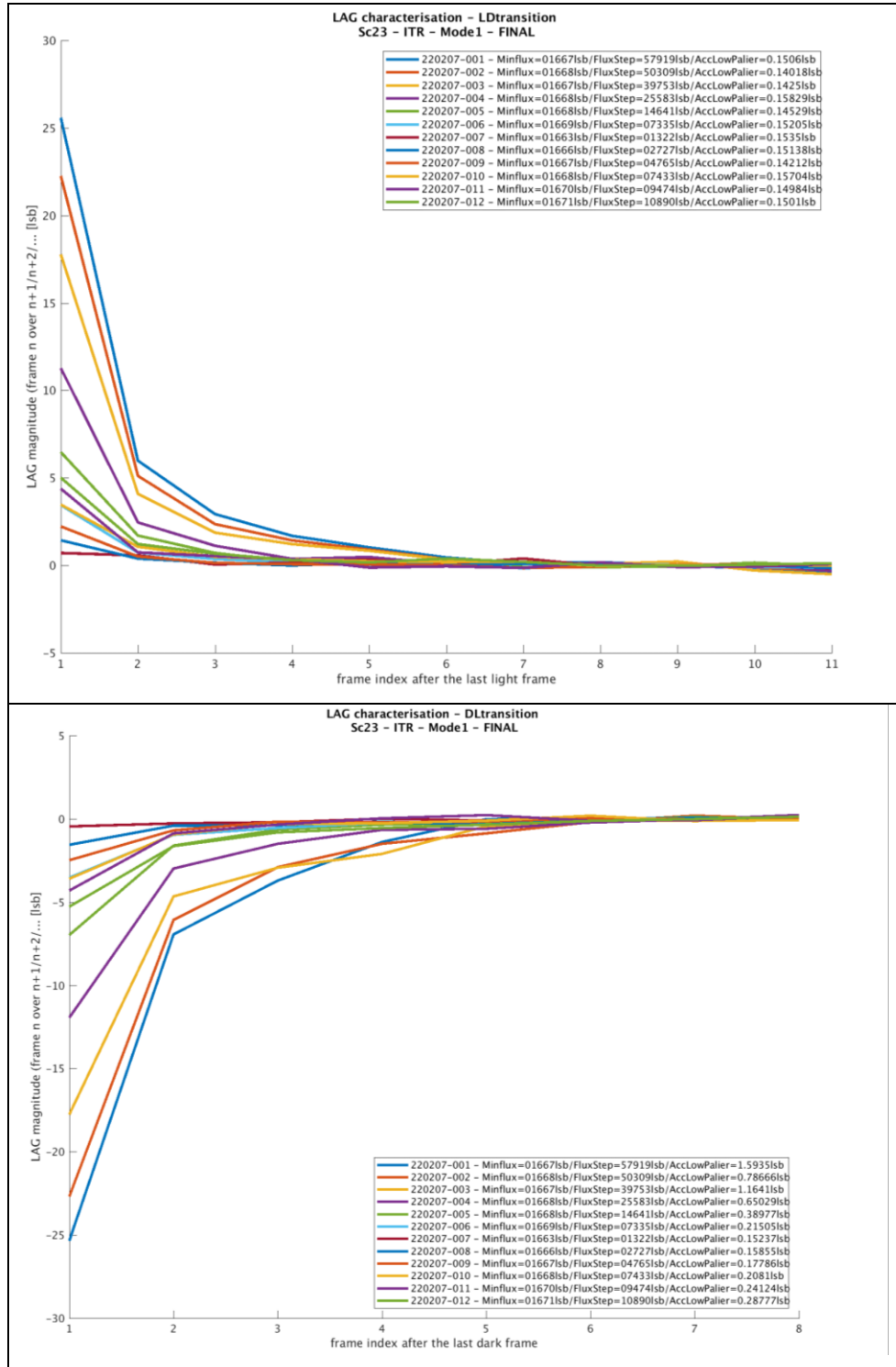


Figure 6. Observed LAG after transition light to dark (top) and transition dark to light (bottom)

6.2 LAG linearity

The following Figure 7, we show another representation of the previous results (Figure 6). We plot the magnitude of the LAG order n as a function of the magnitude of the DL or LD transition. The order n , means the LAG on the frame n after the transition.

The measurement accuracy error (error bars) is assessed to be about 0.2lsb.

We note that for the all the orders, and for the LD and DL transition, the magnitude of the LAG is fully linear with the transition flux. This is a very important characteristic for two reasons:

- A numerical correction is simple to put into a place
- The impact of the phenomenon, at an equivalent magnitude, is for the CO2M mission, much less serious.

In the Table 1, the relative magnitude (ie: the slope of the linear regression model) is summarized. The relative magnitude of the LAG is opposed between a Dark to Light transition and Light to Dark transition, which is consistent with a linear filter model.

Table 1. Relative magnitude of the LAG

LAG	light to dark	dark to light
1-order	0.044%	-0.045%
2-order	0.010%	-0.012%
3-order	0.005%	-0.006%
4-order	0.003%	-0.003%

6.3 LAG numerical model

In view of the characteristics of the LAG showed in the previous section, we have chosen to model the LAG by the following direct model :

$$\forall i,j,n \quad \text{Measure}(i,j,n) = \text{Signal}(i,j,n) + \alpha_1 * \text{Signal}(i,j,n-1) + \alpha_2 * \text{Signal}(i,j,n-2) + \alpha_3 * \text{Signal}(i,j,n-3) + \alpha_4 * \text{Signal}(i,j,n-4) + \alpha_5 * \text{Signal}(i,j,n-5) \quad (1)$$

Where:

- i and j are, respectively, the line and the column index of the detector matrix,
- n is the frame index
- α (s) are the LAG magnitude parameters

Then we will invert this model, and use it as a correction model on real measurements in order to test its consistency.

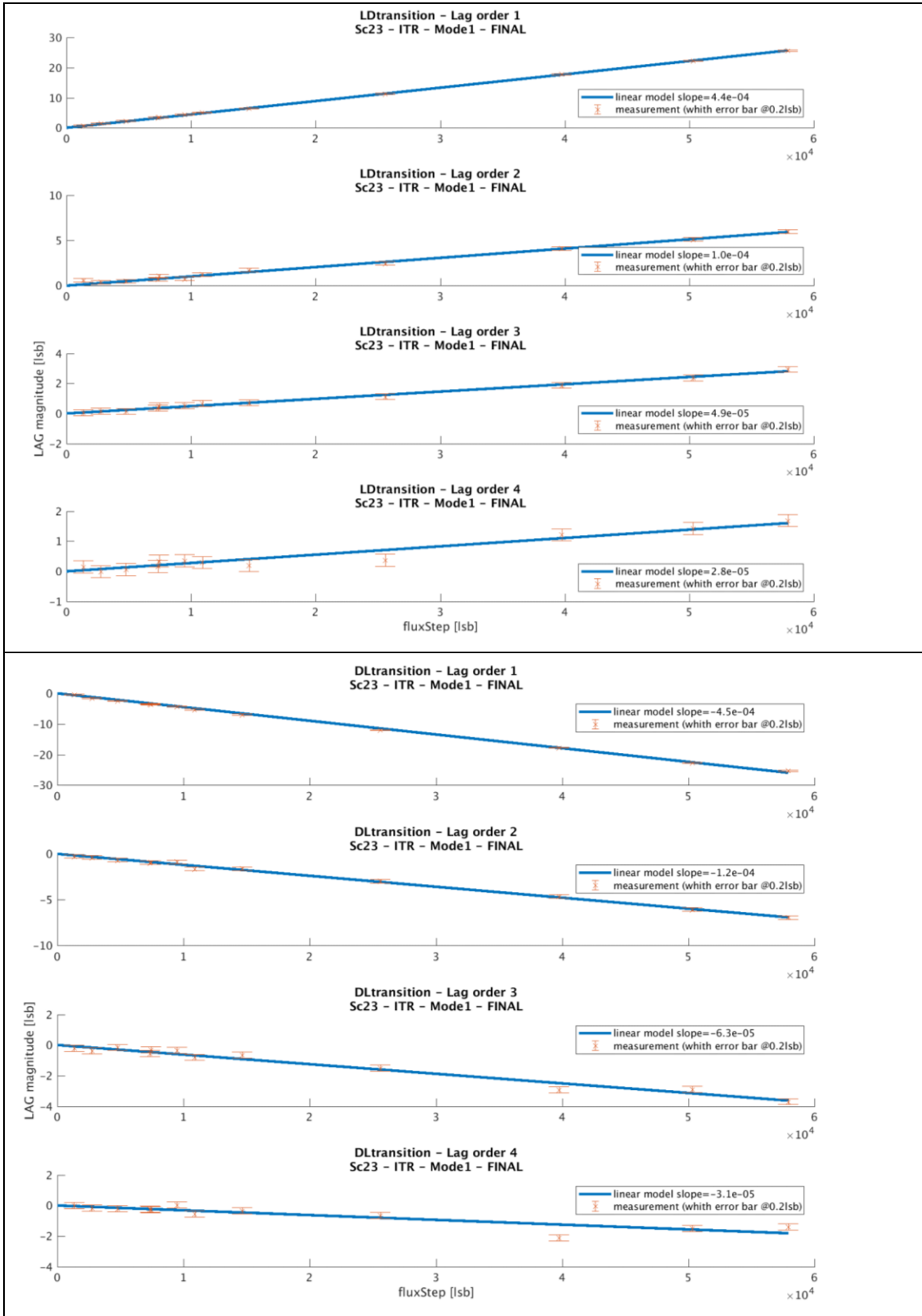


Figure 7. LAG magnitude as a function of the magnitude of the transition flux.

6.4 LAG numerical correction

As whatever i , $\alpha_i \ll 1$, the related correction model is given by the equation (2).

$$\begin{aligned}
 \forall i,j,n \text{Signal}(i,j,n) \approx & \text{Measure}(i,j,n) - \alpha_1 * \text{Measure}(i,j,n-1) \\
 & - \alpha_2 * \text{Measure}(i,j,n-2) \\
 & - \alpha_3 * \text{Measure}(i,j,n-3) \\
 & - \alpha_4 * \text{Measure}(i,j,n-4) \\
 & - \alpha_5 * \text{Measure}(i,j,n-5)
 \end{aligned}
 \tag{2}$$

With

LAG model	
alpha1	0.03350%
alpha2	0.00540%
alpha3	0.00265%
alpha4	0.00156%
alpha5	0.00094%
alpha6	0.00045%

In order to assess the performance of the numerical correction, we use the following method represented in the Figure 8. We used real data, and used the same method of measurement of the LAG in the two branches. The numerical correction model is applied without any knowledge of the illumination scenario or magnitude, as a finite impulse response (FIR) filtering.

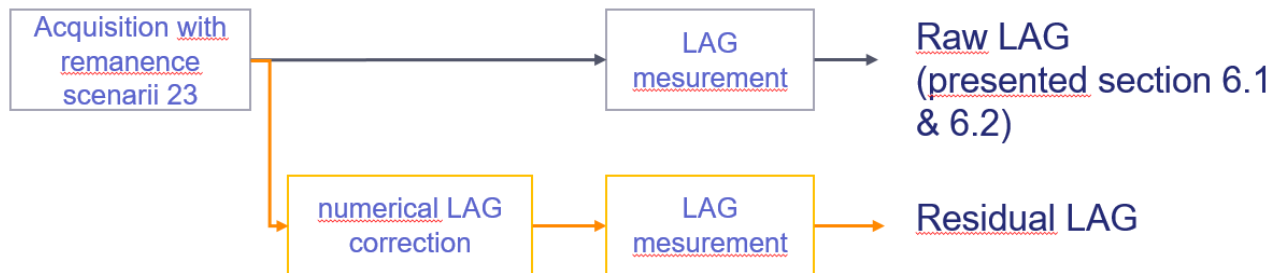


Figure 8. Functional bloc diagram to assess the numerical correction of the LAG

The residual of LAG, measured after the numerical correction of the data, are showed in the Figure 9. The performance of the numerical are very accurate. Starting from a raw magnitude higher than 250e-, the residual of LAG is lower than 10e-, whatever the magnitude of the transition, whatever the transition LD or DL.

Additionally, the LAG being linear and the correction model also being linear, the correction residuals are also totally linear.

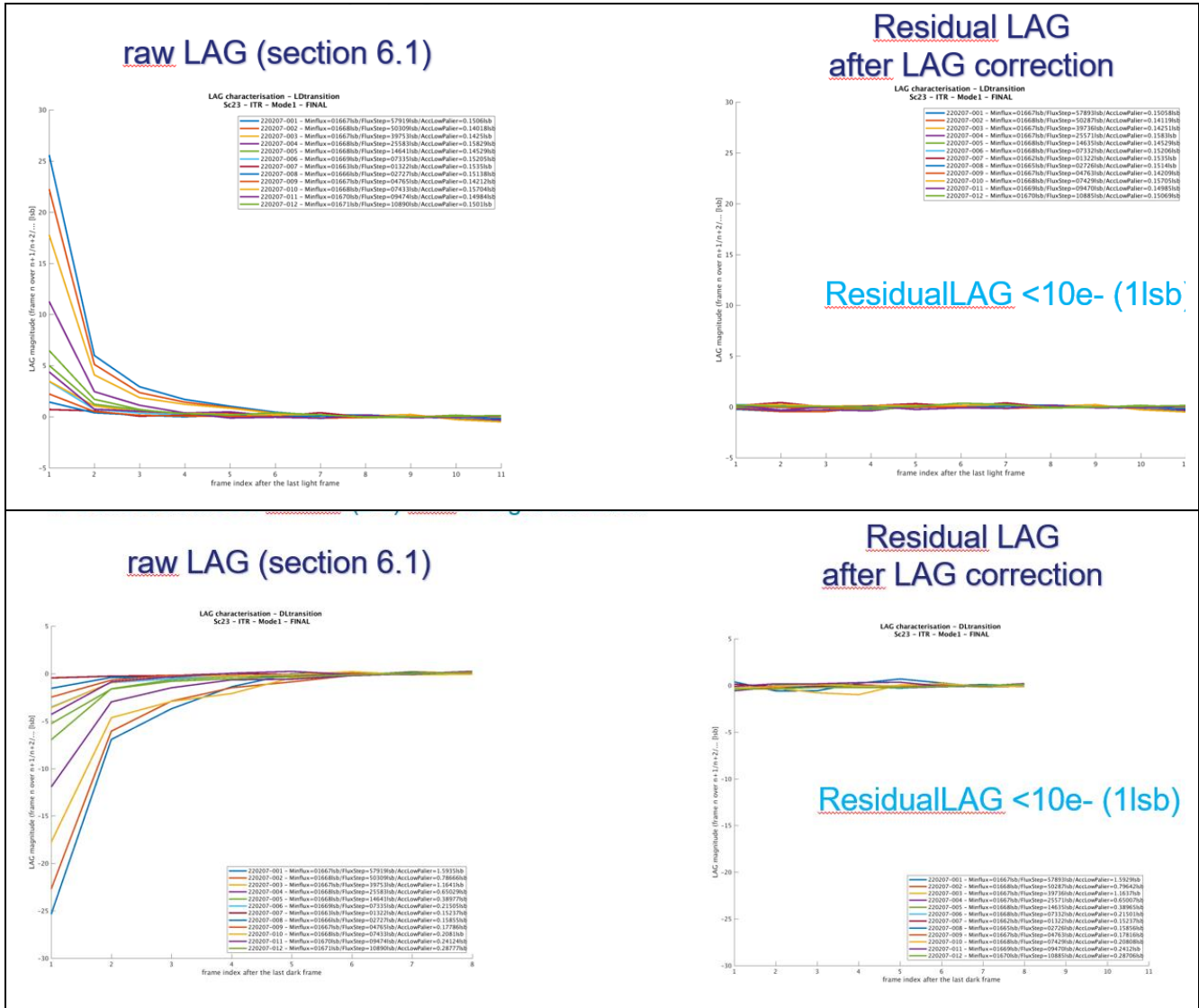


Figure 9. LAG numerical correction assessment

7. CONCLUSION

We presented the results of a remanence characterization on a Lynred NGP detector. This characterization made it possible to identify 3 remanence effects, two linked to the ROIC and one linked to the sensitive layer effect. The first two effects could be completely eliminated by the use of a non-destructive reading for the first, and by a slight increase of the reset time for the second.

The third effect, LAG, has been characterized with a very high accuracy (better than 2electrons). It was found that the LAG was linear with the illumination magnitude, whatever the order of the sample observed. This allowed us to build a numerical correction model that has been tested on real data. We show that the residuals after correction are less than 10 electrons, and, taking into account the particularity of the correction model, are also linear with the flux. This feature of linearity with the flux is very important, especially for the CO2M mission which observes atmospheric lines.

The purpose of this test campaign, and among others the results presented here, made it possible to demonstrate the feasibility of the CO2M mission using the NGP detector.

To go further, concerning the LAG we plan to assess the impact of a variation of illumination during the integration time, that is to say, to measure the impact of heterogeneous scene on the LAG. And, more broadly, other ROIC (intra frame effects) are present that should be analyzed later.

If the measurements and the design of the test bench were made by Thales Alenia Space, this work is part of a collaborative technical work between Thales Alenia Space, Lynred, and the European Space Agency.

REFERENCES

- [1] Bernd Sierk, Valerie Fernandez, J.-L. Bézy, Y. Meijer, Y. Durand, G. Bazalgette Courrèges-Lacoste, C. Pachot, A. Löscher, H. Nett, K. Minoglou, L. Boucher, R. Windpassinger, A. Pasquet, D. Serre, F. te Hennepe, "The Copernicus CO2M mission for monitoring anthropogenic carbon dioxide emissions from space," Proc. SPIE 11852, International Conference on Space Optics — ICSO 2020, 118523M (11 June 2021); <https://doi.org/10.1117/12.2599613>
- [2] Anne Delannoy, Bruno Fièque, Philippe Churier, Céline Riuné, "NGP: a new large format infrared detector for observation, hyperspectral and spectroscopic space missions in VISIR, SWIR and MWIR wavebands," Proc. SPIE 9639, Sensors, Systems, and Next-Generation Satellites XIX, 96390R (12 October 2015); <https://doi.org/10.1117/12.2197239>.
- [3] Simon Tulloch, Elizabeth George, ESO Detector Systems Group, "Predictive model of persistence in H2RG detectors," J. Astron. Telesc. Instrum. Syst. 5(3) 036004 (3 September 2019) <https://doi.org/10.1117/1.JATIS.5.3.036004>.